Photochemistry and Photobiology, 20**, **: *–*

Absorption Characteristics and Quantum Yields of Singlet Oxygen Generation of Thioguanosine Derivatives

Shoma Miyata[1], Takeshi Yamada[1], Tasuku Isozaki[1], Hideyuki Sugimura[1], Yao–Zhong Xu[2] and Tadashi Suzuki[1]*

[1]Department of Chemistry and Biological Science, Aoyama Gakuin University, Sagamihara, Kanagawa, Japan
[2]School of Life, Health and Chemical Sciences, the Open University, Milton Keynes, UK

Received 24 November 2017, accepted 17 January 2018, DOI: 10.1111/php.12900

ABSTRACT

6-Thioguanine (1a) is considered to be photochemotherapeutic due to its specific characteristics of photosensitivity to UVA light and singlet molecular oxygen generation. To extend its phototherapeutic ability, two related thioguanines, 8-thioguanine (2a) and 6,8-dithioguanine (3a), have been designed and explored. Since the solubility of these thioguanines in dehydrated organic solvents is too poor to study, their triacetyl-protected ribonucleosides, that is, 2′,3′,5′-tri-*O*-acetyl-6-thioguanosine (1c), 2′,3′,5′-tri-*O*-acetyl-8-thioguanosine (2c) and 2′,3′,5′-tri-*O*-acetyl-6,8-dithioguanosine (3c) were prepared and investigated. The absorption maxima of 1c, 2c and 3c in acetonitrile were found at longer wavelengths than that of unthiolated guanosine (4c). Especially, 3c has the longest wavelength for absorption maximum and the highest value in terms of molar absorption coefficient among all thionucleobases and thionucleosides reported. These absorption properties were also well reproduced by quantum chemical calculations. Quantum yields of singlet oxygen generation of 2c and 3c were determined by near-infrared emission measurements to be as large as that of 1c. These results suggest that the newly synthesized thioguanosines, in particular 3c, can be further developed as a potential photosensitive agent for light-induced therapies.

INTRODUCTION

6-Thioguanine (**1a**, see Scheme 1) and other thioanalogs of natural nucleobases have high affinity to proliferating cells, and some of them have been prescribed for the treatment of cancers, leukemia and angina among others (1–9). **1a** can be converted into 6-thioguanosine (**1b**) through cellular metabolism, followed by being incorporated into RNA and DNA (1–6,10,11). O'Donovan *et al.* (8) reported that **1a** localizing in tumor cell generated reactive oxygen species (ROS) by its exposure to UVA light and thus cellular apoptosis was induced. These findings indicate that **1a** and its nucleosides could be used as an effective medical tool for cancer treatment due to their unique properties as photochemotherapeutic drugs like 4-thiothymidine, including a photoactivatable genotoxic agent and a photosensitizer for photodynamic therapy (PDT), in addition to the hitherto known use as an anticancer medicine (5,9,12,13).

As a photochemotherapeutic agent, the photosensitizer must be sensitive to the light penetrating into deep hypodermal tissue and can also effectively generate singlet oxygen ($^1O_2$*), one type of ROS. In the ultraviolet and visible light region, the longer wavelength light has higher permeability to subcutaneous tissues (14). However, the absorption maxima of **1a** and **1b** have been observed at around 350 nm, which is not long enough to allow the light to penetrate into deep subcutaneous tissues (2,3,15–19). Thus, it is well worth designing and developing alternative thioguanines and their nucleosides with an absorption band at longer wavelengths.

Photophysical and photochemical properties of **2a**, **3a** and their nucleosides (**2b** and **3b**) have not been documented although their synthetic studies were reported (20–23). 8-Oxoguanine (with a carbonyl group at 8-position of the purine ring and also known as an oxidation photoproduct of guanine (**4a**)) was reported to exhibit a redshifted absorption band relative to its 6-oxo-analogs (**4a** and **4b**) (24–26). In addition to **1a** and **1b**, thiocarbonyl-modified pyrimidine bases (such as thiolated-uracil and thiolated-thymine) have a strong absorption maximum at longer wavelength than their respective unthiolated nucleobases (27–31). Thus, the newly designed thioguanines, especially **3a**, could outstrip the thioanalogs of nucleobases examined so far in terms of their absorption properties. Photochemical experiments should be carried out in rigidly dehydrated organic solvents to clarify the intrinsic property of the excited states for the thionucleobases; however, purine nucleobases have generally low solubility in most of the organic solvents (32). Thus, we prepared triacetyl-protected derivatives (**1c**–**4c**) for better solubility and easier handlings.

In this article, we report our work on chemical synthesis and photochemical investigation of thiolated guanosine derivatives (**1c**, **2c** and **3c**). We also present out results on their structural characterizations by NMR, absorption properties by steady-state absorption spectra and quantum yields of $^1O_2$* generation by time-resolved near-infrared emission measurement. It is our view that these thioguanosine derivatives can be further developed as potential photochemotherapeutic agents.

MATERIALS AND METHODS

General. Reagents were purchased from standard suppliers and used without further purification. Solvents were used after distillation. Reactions were monitored with thin-layer chromatograph (TLC) plate (Silica gel 60, F254). Spots on the TLC plate were monitored with UV,

*Corresponding author email: suzuki@chem.aoyama.ac.jp (Tadashi Suzuki)

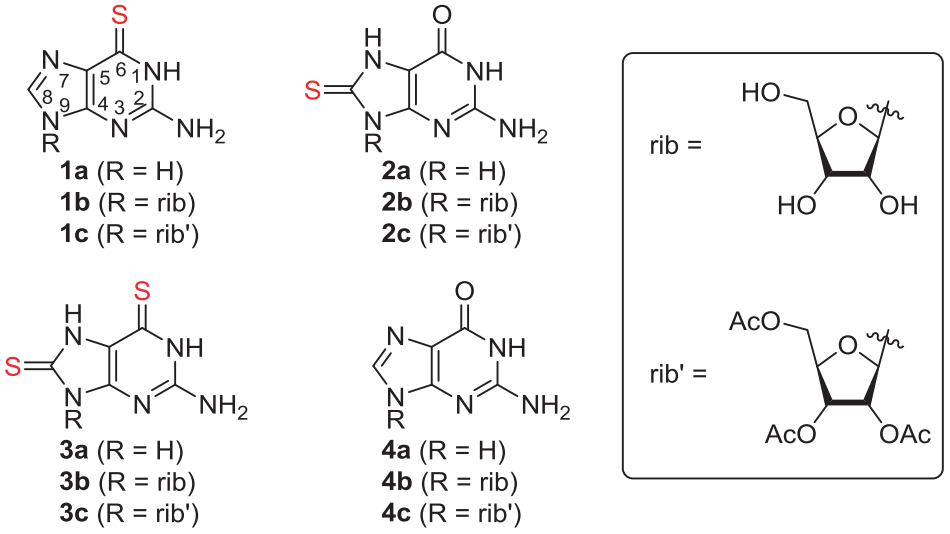

Scheme 1. Structures of guanine, thioguanines and their nucleosides.

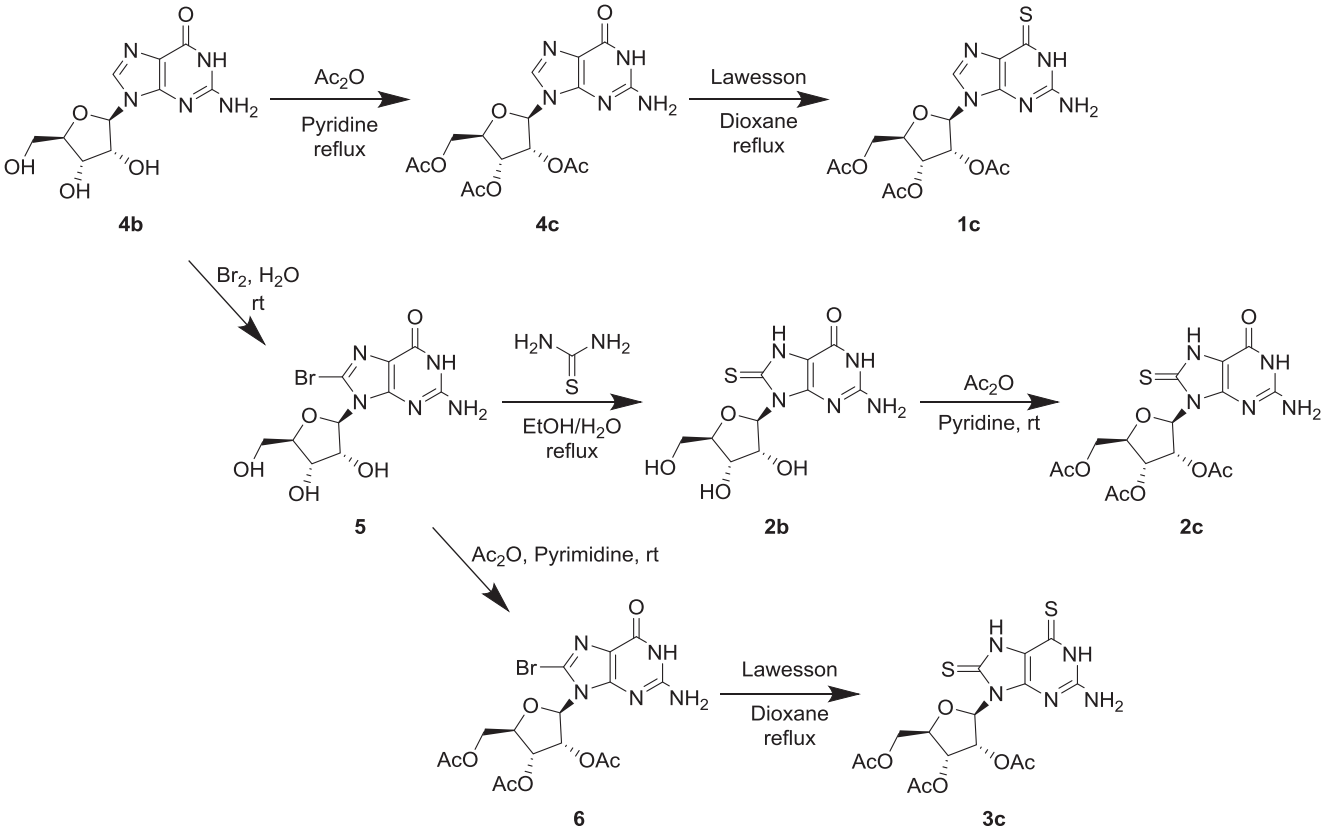

Scheme 2. The synthesis routes for thioguanosines and their acetylated derivatives.

ninhydrin or anisaldehyde. A C–200 silica gel was used for silica gel flash chromatography. ^{1}H NMR and ^{13}C NMR spectra were measured with 500 MHz NMR (JEOL, JNM-ECX 500 MHz), and typical ^{1}H NMR and ^{13}C NMR spectra are shown in the Supporting Information (Figures S1–S8). The multiplicity was expressed as follows: s = singlet, d = doublet, t = triplet, m = multiplet and br = broad. The chemical shifts are expressed in ppm relative to residual solvent as an internal standard, and coupling constants (*J* values) were represented in hertz. Mass spectrum was measured using FAB–MS (JEOL, JMS–700 MStation).

*Synthesis of 2′,3′,5′-tri-O-acetylguanosine (**4c**).* Acetic anhydride (9 mL, 95.2 mmol) was added to a solution of guanosine (**4b**, 2.83 g, 10.0 mmol) in pyridine (27 mL), and the mixture was kept for 2 h at 80°C. The reaction was quenched by addition of H_2O at 0°C after

checking the completion of the reaction by TLC. The reaction mixture was dissolved in ethyl acetate and washed with saturated NH_4Cl, and the organic layer was dried with anhydrous magnesium sulfate. After evaporation of the solvent and column chromatography (CH_2Cl_2/MeOH = 9:1), 2′,3′,5′-tri-*O*-acetylguanosine (**4c**, 2.21 g, 5.40 mmol, 54%) was obtained as white solid. Rf = 0.40 (CH_2Cl_2/MeOH = 9:1): ^{1}H NMR (500 MHz, dimethylsulfoxide–d_6) (δ, ppm) 10.76 (1H, s), 7.89 (1H, s), 6.55 (2H, br s), 5.95 (1H, d, J = 6.2 Hz), 5.75 (1H, t, J = 5.5 Hz), 5.46 (1H, dd, J = 5.8, 4.5 Hz), 4.34 (1H, dd, J = 13.8, 4.1 Hz), 4.29–4.26 (1H, m), 4.22 (1H, dd, J = 11.7, 5.5 Hz), 2.07 (3H, s), 2.00 (3H, s) and 1.86 (3H, s); ^{13}C NMR (125 MHz, dimethylsulfoxide–d_6) (δ, ppm) 170.6, 170.0, 169.8, 157.2, 154.5, 151.6, 136.2, 117.3, 84.9, 80.1, 72.6, 70.8, 63.6, 21.1, 20.9 and 20.7.

*Synthesis of 2′,3′,5′-tri-O-acetyl-6-thioguanosine (**1c**).* Lawesson's reagent (1.19 g, 2.93 mmol) was added to a solution of 2′,3′,5′-tri-*O*-acetylguanosine (**4c**, 2.01 g, 4.91 mmol) in dioxane (40 mL), and the mixture was kept for 5 h at +100°C. The reaction mixture was dissolved in ethyl acetate and washed with saturated $NaHCO_3$, and the organic layer was dried with anhydrous magnesium sulfate. After evaporation of the solvent and column chromatography (CH_2Cl_2/MeOH = 97:3), 2′,3′,5′-tri-*O*-acetyl-6-thioguanosine (**1c**, 0.999 g, 2.35 mmol, 48%) was obtained as white solid. Rf = 0.51 (CH_2Cl_2/MeOH = 9:1): ^{1}H NMR (500 MHz, dimethylsulfoxide–d_6) (δ, ppm) 12.03 (1H, s), 8.09 (1H, s), 6.84 (2H, s), 5.95 (1H, d, J = 6.2 Hz), 5.76 (1H, t, J = 6.2 Hz), 5.45 (1H, dd, J = 6.2, 4.1 Hz), 4.34 (1H, dd, J = 11.3, 3.7 Hz), 4.30 (1H, dd, J = 9.6, 4.1 Hz), 4.23 (1H, dd, J = 11.0, 5.5 Hz), 2.07 (3H, s), 2.00 (3H, s) and 1.99 (3H, s); ^{13}C NMR (125 MHz, dimethylsulfoxide–d_6) (δ, ppm) 176.0, 170.0, 169.9, 169.8, 153.7, 148.2, 139.0, 128.9, 85.1, 80.2, 72.5, 70.8, 63.5, 21.1, 20.9 and 20.7.

*Synthesis of 8-bromoguanosine (**5**).* Br_2 (3.0 mL) was added to a suspension liquid of guanosine (**4b**, 5.0 g, 17.7 mmol) in H_2O (100 mL), and the vigorous stirring was kept for 24 h at room temperature. Excess Br_2 was quenched by addition of saturated sodium thiosulfate solution (3.0 mL); the precipitate was collected by filtration and washed by H_2O on a Buchner funnel. After evaporation of the solvent, 8-bromoguanosine (**5**, 6.3 g, 17.5 mmol, 99%) was obtained as white solid.

*Synthesis of 8-thioguanosine (**2b**).* Thiourea was added to a suspension liquid of 8-bromoguanosine (**5**, 4.01 g, 11.1 mmol) in ethanol (40 mL). A small quantity of H_2O (5 mL) was added until the suspension liquid being dissolved and kept heated to reflux for 24 h. The reaction mixture was cooled at room temperature, excess ethanol was evaporated, and the precipitated solid was filtered. The solid was washed with H_2O on a Buchner funnel, and after evaporation of the solvent, 8-thioguanosine (**2b**, 2.39 g, 7.59 mmol, 68%) was obtained as white solid.

*Synthesis of 2′,3′,5′-tri-O-acetyl-8-thioguanosine (**2c**).* Acetic anhydride (2 mL, 21.2 mmol) was added to a solution of 8-thioguanosine (**2b**, 2.10 g, 6.69 mmol) in pyridine (35 mL), and the mixture was kept for 8 h at room temperature. The reaction was quenched by addition of H_2O at 0°C after checking the completion of the reaction by TLC. The reaction mixture was dissolved in ethyl acetate and washed with saturated NH_4Cl, and the organic layer was dried with anhydrous magnesium sulfate. After evaporation of the solvent and column chromatography (CH_2Cl_2/MeOH = 95:5), 2′,3′,5′-tri-*O*-acetyl-8-thioguanosine (**2c**, 1.76 g, 3.98 mmol, 59%) was obtained as white solid. Rf = 0.46 (CH_2Cl_2/MeOH = 9:1): ^{1}H NMR (500 MHz, dimethylsulfoxide–d_6) 13.02 (1H, br), 11.09 (1H, br), 6.62 (2H, br), 6.38 (1H, s), 6.10 (1H, br), 5.63 (1H, t, J = 6.0 Hz), 4.38 (1H, dd, J = 11.7, 3.4 Hz), 4.20 (1H, m), 4.17 (1H, dd, J = 11.3, 6.5 Hz) 2.06 (3H, s), 2.02 (3H, s) and 1.97 (3H, s); ^{13}C NMR (125 MHz, dimethylsulfoxide–d_6) 170.7, 169.88, 169.82, 165.5, 154.4, 151.4, 149.7, 104.4, 86.8, 79.5, 71.3, 70.7, 63.5, 21.0, 20.8 and 20.7.

*Synthesis of 2′,3′,5′-tri-O-acetyl-8-bromoguanosine (**6**).* Acetic anhydride (5 mL, 52.9 mmol) was added to a solution of 8-bromoguanosine (**5**, 4.76 g, 13.2 mmol) in pyridine (29 mL), and the mixture was kept for 6 h at room temperature. The reaction was quenched by addition of H_2O at 0°C after checking the completion of the reaction by TLC. The reaction mixture was dissolved in ethyl acetate and washed with saturated NH_4Cl, and the organic layer was dried with anhydrous magnesium sulfate. After evaporation of the solvent and column chromatography (CH_2Cl_2/MeOH = 95:5), 2′,3′,5′-tri-*O*-acetyl-8-bromoguanosine (**6**, 4.79 g, 9.84 mmol, 75%) was obtained as white solid. Rf = 0.48 (CH_2Cl_2/MeOH = 9:1).

*Synthesis of 2′,3′,5′-tri-O-acetyl-6,8-dithioguanosine (**3c**).* Lawesson's reagent (8.75 g, 21.6 mmol) was added to a solution of 2′,3′,5′-tri-*O*-acetyl-8-bromoguanosine (**6,** 5.00 g, 10.3 mmol) in dioxane (100 mL), and the mixture was kept for 4 h at +100°C. The reaction mixture was dissolved in ethyl acetate and washed with saturated $NaHCO_3$, and the organic layer was dried with anhydrous magnesium sulfate. After evaporation of the solvent and column chromatography (CH_2Cl_2/MeOH = 97:3), 2′,3′,5′-tri-*O*-acetyl-6,8-thioguanosine (**3c**, 2.33 g, 5.10 mmol, 50%) was obtained as yellow solid. Rf = 0.54 (CH_2Cl_2/MeOH = 9:1): ^{1}H NMR (500 MHz, dimethylsulfoxide–d_6) 13.11 (1H, br), 12.21 (1H, br), 6.93 (2H, br), 6.40 (1H, d, J = 4.1 Hz), 6.08 (1H, t, J = 5.5 Hz), 5.60 (1H, t, J = 6.2 Hz), 4.38 (1H, dd, J = 11.7, 6.9 Hz), 4.22 (1H, m), 4.16 (1H, dd, J = 11.7, 6.9 Hz), 2.06 (3H, s), 2.02 (3H, s) and 1.97 (3H, s); ^{13}C NMR (125 MHz, dimethylsulfoxide–d_6) 170.6, 169.88, 169.84, 168.1, 164.1, 154.1, 146.7, 117.8, 86.8, 79.6, 71.1, 70.7, 63.5, 21.1, 20.8, 20.7: MS (FAB+) m/z 458 (MH^+).

Ultraviolet–visible (UV–vis) absorption spectroscopy. The UV–vis absorption spectra were recorded at room temperature on a spectrophotometer (JASCO, U–best V550) using a quartz cuvette of 1 cm optical path length. The sample solution was prepared with acetonitrile as a solvent.

Time-resolved near-infrared emission spectroscopy. Time-resolved near-infrared emission measurement was carried out with a thermoelectric cooled near-infrared photomultiplier tube (Hamamatsu Photonics, H10330–45; InP/InGaAsP, spectral response 950–1400 nm) combined with a long-pass filter (Thorlabs, FEL1250; cut-on wavelength 1250 nm) and a bandpass filter (Edmund, Hard-coated bandpass filter; 1275 ± 50 nm) (Figure S9). A forth-harmonic of a Nd^{3+}:YAG laser (Continuum, Surelite II–10, 5 ns pulse duration, 10 Hz, 266 nm) was used as an excitation light source. The sample solution was prepared with acetonitrile as a solvent.

Quantum chemical calculation. Ground- and excited-state calculations for corresponding purine bases (**1a**–**4a**) were performed using the Gaussian 09W program package (33). Ground-state geometries of the purine bases were optimized by the density functional theory (DFT) at the B3LYP/6−311 + G(d,p) level. Vertical excitation energies were estimated by the time-dependent DFT (TD-DFT) at the TD−B3LYP/6−311 + G(d,p) level. Solvent effects were modeled with the polarizable continuum model (PCM) for the ground and excited states.

RESULTS AND DISCUSSION

Synthesis of thioguanosine derivatives

Scheme 2 outlines the synthetic routes to **1c**–**4c**. The syntheses of **1c**, **2c** and **4c** have been reported previously (34–43). To the best of our knowledge, this is the first report on chemical synthesis of **3c**. The structures of all synthesized products were characterized by ^{1}H NMR, and their purities were estimated to be 99% for **1c**, 99% for **2c**, 99% for **3c** and 97% for **4c** with a minor amount of impurity being H_2O. The concentration of H_2O was determined by subtracting the peak area deriving from H_2O in dimethylsulfoxide–d_6 solvent from that in **1c**–**4c** solutions to remove the intrinsic moisture content of the deuterated solvent. No other impurity was detected by HPLC spectra as shown in Figure S10.

1c was prepared in a two-step process for the first time. First, **4b** was quantitatively converted to **4c**, which then was transformed to **1c** with Lawesson's reagent. Following the reported procedure (20,42,43), **2c** was synthesized in a three-step process from **4b**. To prepare **3c**, **6** is the key intermediate which can be obtained from bromination of **4b** followed by acetylation of the resultant **5** in an excellent yield (22,43). In an early report (22), **6** had been treated with phosphoryl chloride and hydrolyzed to afford 2-amino-6,8-dichloropurine, followed by nucleophilic substitution reaction with thiourea to yield **3b**. In order to overcome the difficulty in handling the phosphoryl chloride and its low yield of **3b** (33%) (22), thus, we developed another synthetic route to **3c**. By a simple treatment of **6** with Lawesson's reagent, **3c** was successfully afforded with a higher yield of 50%.

Table 1. ^{1}H NMR chemical shifts of **1c**–**4c**.

	N^1H	N^7H	N^2H_2	1′	2′	3′	4′	5′	5′
1c	**12.03**	–	**6.84**	5.95	5.76	5.45	4.30	4.34	4.23
2c	**11.09**	13.02	6.62	**6.38**	6.10	5.63	4.20	4.38	4.17
3c	**12.21**	13.11	**6.93**	**6.40**	6.08	5.60	4.22	4.38	4.16
4c	10.76	–	6.55	5.95	5.75	5.46	4.27	4.34	4.22

Bold values are the values that are noticeably high due to the effect of the thiocarbonyl modification in these compounds.

^{1}H and ^{13}C NMR analysis of thioguanosine derivatives

To ascertain the correct structures of the synthesized products, NMR spectroscopy was used. The ^{1}H NMR chemical shifts of **1c**–**4c** are listed in Table 1. The chemical shift values for the proton at 1-position (the imide group) of thioguanosine derivatives were observed at lower magnetic field than that of unthiolated guanosine. The peaks for the imide group, especially in **1c** and **3c**, were significantly shifted to a lower magnetic field. This shift can be ascribed to the thiocarbonyl substitution at 6-position of the purine ring. The thiocarbonyl modification at 8-position also causes a significant shift of the peak for the imide group to a lower magnetic field, as observed for **2c**. The peaks for the amine protons at 2-position of the purine ring for **1c** and **3c** also exhibited a slight shift to the low field in comparison with the corresponding peak for **2c** and **4c**. The chemical shift values deriving from ribose sugar protons, especially for anomeric proton (1′H), were also shifted to a lower magnetic field in both **2c** and **3c**. These shifts can be ascribed to the thiocarbonyl modification at 8-position, consistent with a recent publication in which the peak for the proton at 3-position (the imide group) in 4-thiopyrimidines was also found to be at lower magnetic field than that of unthiolated pyrimidine bases (44).

Table 2 lists ^{13}C NMR chemical shifts of all the carbon atoms in compounds **1c**–**4c**. The peak at 157.2 ppm in unthiolated **4c** was found to shift to 176.0 ppm (18.8 ppm lower magnetic field) in the 6-thiolated analog (**1c**). Similarly, the peak at 136.2 ppm in the unthiolated **4c** was also found to shift substantially to 165.5 ppm in the 8-thiolated analog (**2c**), resulting 29.3 ppm lower magnetic field shift. Compound **3c** is a doubly thiolated analog, both of the thiocarbonyl carbons are shifted to a lower field (*i.e.* 168.1 and 164.1 ppm) compared with those of unthiolated **4c**. These shifts should be due to the thiolation at their respective positions (6-position and 8-position). The similar effect was also reported for the carbon atoms of thiocarbonyl carbons in 2-thiouracil and 4-thiouracil (44,45).

UV–vis absorption spectroscopy

The absorption spectra of **1c**, **2c**, **3c** and **4c** are shown in Fig. 1a. Absorption spectrum of **4c**, appeared in the spectral range less than 295 nm, was almost identical to that of guanosine (**4b**), revealing that the acetylation of three hydroxyl groups in the sugar component had little effect on electronic states concerning with transitions in this spectral range. Since the solubility of **4c** (triacetyl-protected guanosine) in acetonitrile was over 300 times larger than that of **4b** (unprotected guanosine) in units of molarity (16.5 mM for **4c** and 41.6 μM for **4b**), thus corresponding triacetyl-protected analogs instead of the unprotected analog were used to study their UV properties. The absorption spectrum for **2c** (8-thiolated analogy) exhibited an intense absorption band centered at 302 nm with a high molar absorption coefficient [$\varepsilon_{2c}^{302\text{nm}} = (2.39 \pm 0.01) \times 10^4$ M^{-1} cm^{-1}]. In comparison with **4c**, this redshift of the band (48 nm) observed from **2c** is likely to result from the extension of the π-conjugation due to the thiocarbonyl modification at 8-position of the purine ring. **1c** (6-thiolated analogy) has a much large redshifted band (91 nm) with a higher molar absorption coefficient [$\varepsilon_{1c}^{346\text{nm}} = (2.82 \pm 0.01) \times 10^4$ M^{-1} cm^{-1}]. The absorption maximum of **1c** appeared in the longer wavelength region than that of **2c**, indicating that thiocarbonyl modification at 6-position has more contribution to its electronic transition than that at 8-position. Our findings offer a solid support to an early report (17) that the replacement of an oxygen atom by a sulfur atom in a carbonyl group is expected to

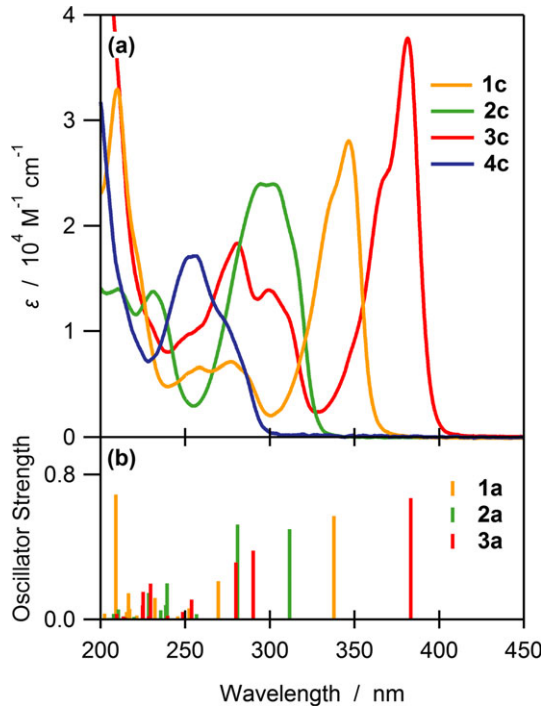

Figure 1. (a) Absorption spectra of **1c**–**4c** in acetonitrile solution, and (b) computational vertical transition energy and oscillator strength of **1a**–**4a** at PCM/TD–B3LYP/6–311G+(d,p) level.

Table 2. ^{13}C NMR chemical shifts of **1c**–**4c**.

	C^2	C^4	C^5	C^6	C^8	1′	2′	3′	4′	5′
1c	153.7	148.2	128.9	**176.0**	139.0	85.1	80.2	72.5	70.8	63.5
2c	151.4	154.4	104.4	149.7	**165.5**	86.8	79.5	71.3	70.7	63.5
3c	146.7	154.1	117.8	**168.1**	**164.1**	86.8	79.6	71.1	70.7	63.5
4c	154.5	151.6	117.3	157.2	136.2	84.9	80.1	72.6	70.8	63.6

Bold values are the values that are noticeably high due to the thiolation at the respective positions in these compounds.

Table 3. Photophysical properties of **1c**, **2c** and **3c** in acetonitrile solution.

	Experimental				Computational‡‡		
	λ_{max}*/nm	ε_{max}†/10^4 M^{-1} cm^{-1}	E_T ‡/eV	Φ_Δ§	E_s¶/nm	f **	E_T††/eV
1c	346	2.82 ± 0.01	2.71	0.37 ± 0.01	338	0.571	2.70
2c	302	2.39 ± 0.01	2.93	0.28 ± 0.01	312	0.497	3.04
3c	**381**	**3.76 ± 0.02**	2.50	0.33 ± 0.01	383	0.669	2.43

*Wavelength at absorption maximum. †Molar absorption coefficient at absorption maximum. ‡Triplet state energy obtained from emission peak of phosphorescence spectrum. §Quantum yield of singlet oxygen generation. ¶Vertical transition energy. **Oscillator strength. ††Triplet state energy. ‡‡Calculated at the PCM/TD–B3LYP/6–311 + G(d,p) level. Bold values are the values that are substantially high due to the thiolation at both 6-position and 8-positions of the compound.

shift the absorption band to the red. The absorption maximum of **3c** (dithiolated analog) was observed at 381 nm, which surprisingly results in a redshift up to 126 nm in comparison with **4c**. In addition, the absorption intensity at the maximum [ε_{3c}^{381nm} = (3.76 ± 0.02) × 10^4 M^{-1} cm^{-1}] was remarkably higher than any other thioanalogs of nucleobases examined so far (2,3,15–18,27–31), revealing **3c** can be activated with a very low dose of UV light. These desirable UV properties suggest that **3c** would be much sensitive to the light penetrating into the human skin and could be used as a powerful photosensitive agent for light-induced therapies, including PDT. Thioguanosines (**1c**, **2c** and **3c**) are not regarded as suitable agents for PDT because of the absence of *one-photon* absorption at visible light. However, in our recent works (46,47), **1b** and **3c** were successfully excited at red light by *multiphoton* excitation. Thus, with the *multiphoton* approach, thioguanosines have offered a potential as a PDT sensitizer.

Steady-state emission measurements were also carried out on **1c**–**3c**, but no emission was observed at room temperature, indicating a fluorescence quantum yield of virtually zero. On the other hand, an emission was clearly observed at 77 K in glassy ethanol matrix, as described in the supporting materials (Figure S11). Those emission bands exhibited significantly large Stokes shift from those absorption maxima (beyond 100 nm, as listed in Table 3) with longer lifetimes, over a microsecond. The emission spectrum of **1c** was identical to the reported phosphorescence spectrum of **1b** (3,48). Although the quantum yields of triplet formation for these thioguanosines (**1c**, **2c** and **3c**) have not been obtained yet, their triplet–triplet absorption spectra were observed at room temperature, which will be described in detail in the next paper. In addition, these thioguanosines have relatively high quantum yields of singlet molecular oxygen generation (see below), indicating high triplet formation of these compounds. Therefore, those emissions can be confidently assigned to their respective phosphorescence of **1c**–**3c**. Thus, **2c** and **3c** as well as **1a**–**1c** will form the excited triplet manifold through intersystem crossing from the singlet excited states.

Quantum chemical calculations

Optimized ground-state geometries of **1a**, **2a** and **3a** are shown in Figure S12 and Tables S1–S3. These molecules belong to the C_s symmetry, and all atoms lie in a plane of the purine ring. The bond lengths and angles were comparable to each other except for the C^6=S and C^6=O bond lengths. The C^6=S bond lengths of **1a** and **3a** (1.69 Å) were significantly larger than the C^6=O bond lengths of **2a** and **4a** (1.23 Å). This clearly reveals that the strength of the C^6=S bond is weaker than that of the C^6=O bond.

Computational vertical transition energies and oscillator strengths of **1a**–**3a** are shown in Fig. 1b and listed in Table 3.

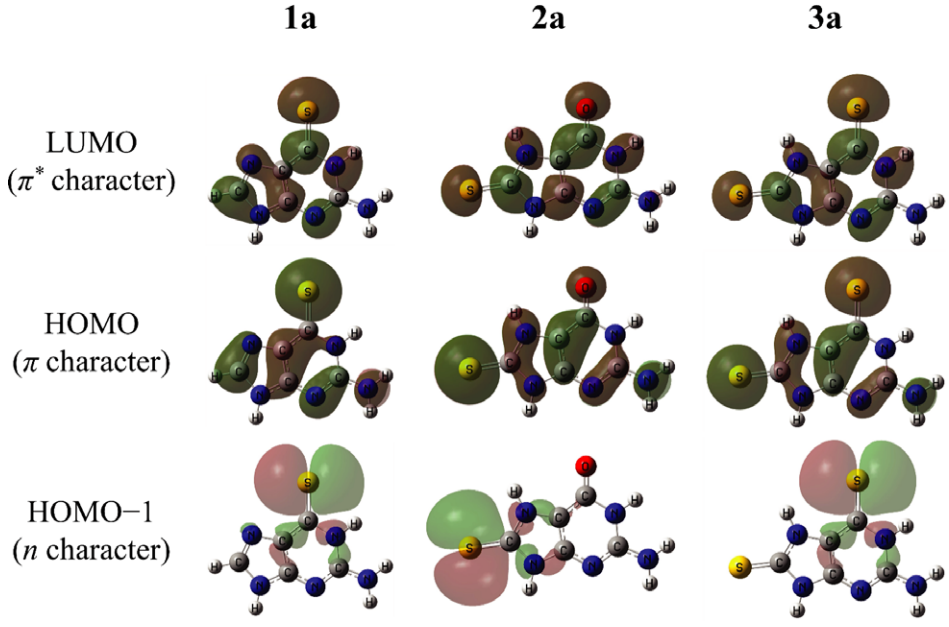

Figure 2. Molecular orbitals involved in transitions to the first and second excited single states of **1a**, **2a** and **3a**.

The calculated vertical transition energies and oscillator strengths of **1a**–**3a** well reproduce the redshifted absorptions of **1c**–**3c** in comparison with **4c**.

Molecular orbitals involved in the transitions to first and second excited singlet states of **1a**–**3a** are shown in Fig. 2. In all compounds, HOMO–1 has *n* characters with electronic density localized around the sulfur atom perpendicularly to the molecular plane, whereas both HOMO and LUMO have π and π^* characters with extended electronic density throughout the molecular plane, respectively. For **1a**, the first excited singlet (S_1) state arises from the transition from the *n* orbital localized on the sulfur atom (HOMO–1) to the π^* orbital (LUMO), and the calculated small oscillator strength ($f < 0.0001$) indicates the forbidden $S_1(n\pi^*) \leftarrow S_0$ transition. On the other hand, the transition to the second excited singlet (S_2) state is allowed $\pi\pi^*$ transition (HOMO → LUMO) ($f = 0.571$). Thus, the intense absorption band of **1c** around 346 nm would be attributed to the $S_2(\pi\pi^*) \leftarrow S_0$ transition. For **2a** and **3a**, the transition to the S_1 and S_2 states arises from the allowed $\pi\pi^*$ transition (HOMO → LUMO) and forbidden $n\pi^*$ transition (HOMO–1 → LUMO). Thus, the absorption peak at the longest wavelength of **2c** and **3c** would be attributed to the $S_1(\pi\pi^*) \leftarrow S_0$ transition. The π and π^* orbitals of **2a** and **3a** were widely extended to the 8-position of the purine ring as shown in Fig. 2, resulting in the redshifted absorption of **2c** and **3c** with respect to **4c** and **1c**, respectively.

For **1a**–**3a**, the T_1 state was also optimized and shown in Figure S13 and Tables S4–S6. The optimized structures for **1a**–**3a** at the T_1 state are also comparable to that at ground-state except for the S^6 atom of **1a** at the T_1 state (only the S^6 atom is out of molecular plane). The optimized structures for **1a**–**3a** at the T_1 state can be assigned to the $\pi\pi^*$ state, as shown in Figure S14. The T_1 state energies of **1a**–**3a** are listed in Table 3. The calculated T_1 energies well agree with the experimental values, estimated from the maximum emission wavelength in the phosphorescence spectra of **1c**–**3c**.

Time-resolved near-infrared emission spectroscopy

The quantum yield of singlet oxygen generation for the thioguanosines was determined for exploration of these potential drugs in photochemotherapy. Figure 3a shows the decay profiles of singlet oxygen phosphorescence measured at around 1275 nm by photosensitization with **1c**, **2c** and **3c** in O_2-saturated acetonitrile solutions. All signals decayed mono-exponentially, and their lifetimes were about 65 μs, well agreeing to the lifetime of $^1O_2$* in acetonitrile (49,50). Since this signal was not detectable in Ar-saturated solutions, the emission should be due to $^1O_2$*, generated by photosensitization with thioguanosines.

The quantum yields of $^1O_2$* generation of thioguanosines were determined in O_2-saturated acetonitrile solutions relative to optically matched phenalenone (PN) solution ($\Phi_\Delta = 1.00 \pm 0.03$) (51). Individual phosphorescence traces were fitted using a single-exponential function to estimate the emission intensity maxima immediately after laser irradiation (I_s^0). The I_s^0 value was plotted against the laser fluence (I_L) (Fig. 3b). A good linear relationship was observed between I_s^0 and I_L. This finding reveals that $^1O_2$* was generated by one-photon process through photosensitization by thioguanosines. The values of the slope obtained from these plots (I_s^0/I_L) were plotted against the ground-state absorptance at excitation wavelength ($1–10^{-A}$), as shown in Fig. 3c. These plots also show good linear relationships. By comparing the slopes of

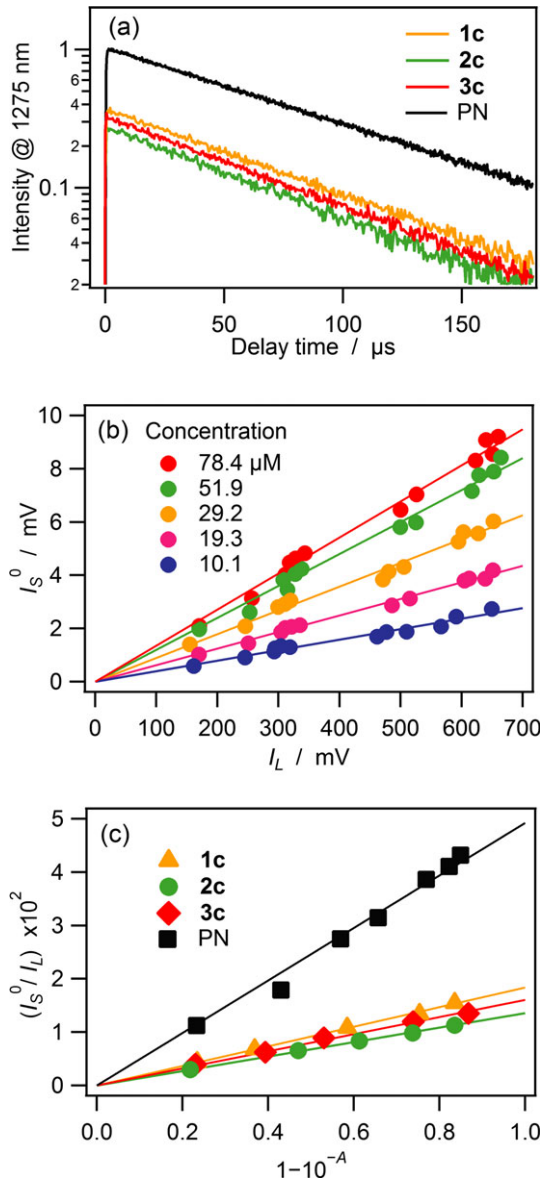

Figure 3. (a) Decay profiles of singlet oxygen phosphorescence measured at around 1275 nm of thioguanosines and PN in acetonitrile solution. Signals are corrected for absorptance at excitation wavelength (266 nm) and incident laser power. (b) Plots of the emission intensity maxima (I_S^0) immediately after laser irradiation in **3c** solutions against incident laser power (I_L), and (c) plots of the I_S^0/I_L value of **1c**, **2c**, **3c** and PN against the absorptance ($1–10^{-A}$) at excitation wavelength (266 nm).

thioguanosines with that of PN, we were able to determine Φ_Δ values, with a high degree of accuracy, as 0.37 ± 0.01 for **1c**, 0.28 ± 0.01 for **2c** and 0.33 ± 0.01 for **3c**. The Φ_Δ value for **1c** was close to those for **1a** and **1b** in the previous report (18,19). These results further confirm that those thioguanosines generate $^1O_2$* effectively through photosensitization.

It was noted that there are only very small differences in the Φ_Δ values among the thioguanosines (see Table 3). $^1O_2$* is considered to generate through energy transfer from the T_1 state of donor molecule to an oxygen molecule ($X^3\Sigma_g^-$) as an energy acceptor by collision each other, thus the Φ_Δ value should depend on the following factors: the intersystem crossing

quantum yield, the triplet lifetime of the sensitizer and the S_Δ value (a fraction of the triplet states quenched by dissolved oxygen which gives rise to singlet oxygen formation). Generally, triplet states of $\pi\pi^*$ have been reported to give a S_Δ value of a range of 0.7–1.0, whereas it is ~0.3 for $n\pi^*$ triplet states (52). All the T_1 state of **1c**, **2c** and **3c** have $\pi\pi^*$ character in the Franck–Condon region obtained by the TD–DFT calculation, and its T_1 energies are large enough to surpass vertical transition energy of oxygen molecules (0.97 eV; $a^1\Delta_g \leftarrow X^3\Sigma_g^-$), as discussed above. Therefore, the differences in Φ_Δ will depend on the lifetime of each T_1 state and/or quantum yields of intersystem crossing to triplet manifolds. To gain the more detailed information on the triplet state such as lifetime and quantum yield, time-resolved spectroscopy is under way.

CONCLUSION

Three novel thioguanosine derivatives (**1c**–**3c**) have been successfully synthesized and characterized by various spectroscopies. The absorption bands of these thioguanosines are found to be at longer wavelengths than those of unthiolated guanosines (**4b** and **4c**). Especially, **3c** has the most redshifted band with a large molar absorption coefficient, indicating that **3c** is much more sensitive to the light penetrating into the human skin. The redshifted spectra for thioanalogs were well reproduced with the quantum chemical calculations. The T_1 character was found to be a $\pi\pi^*$ character. In addition, the thioguanosines generated $^1O_2^*$ effectively through photosensitization (Φ_Δ = 0.28–0.37). Taken together, these results clearly show that our reported thioguanosines have some potential for photochemotherapy, as a photoactivatable genotoxic agent and/or a photosensitizer for PDT. Although the S_Δ value for the T_1 ($\pi\pi^*$) was known to be high, the small difference in Φ_Δ values among the thioguanosines is likely to be dependent on the intersystem crossing quantum yield and/or T_1 state lifetime of each individual thioguanosine.

SUPPORTING INFORMATION

Additional Supporting Information may be found in the online version of this article:

Figure S1. ^{1}H NMR spectrum of **1c** in dimethylsulfoxide–d_6 solution.

Figure S2. ^{13}C NMR spectrum of **1c** in dimethylsulfoxide–d_6 solution.

Figure S3. ^{1}H NMR spectrum of **2c** in dimethylsulfoxide–d_6 solution.

Figure S4. ^{13}C NMR spectrum of **2c** in dimethylsulfoxide–d_6 solution.

Figure S5. ^{1}H NMR spectrum of **3c** in dimethylsulfoxide–d_6 solution.

Figure S6. ^{13}C NMR spectrum of **3c** in dimethylsulfoxide–d_6 solution.

Figure S7. ^{1}H NMR spectrum of **4c** in dimethylsulfoxide–d_6 solution.

Figure S8. ^{13}C NMR spectrum of **4c** in dimethylsulfoxide–d_6 solution.

Figure S9. Schematic diagram of the experimental setup for the time–resolved near IR emission measurement.

Figure S10. HPLC chart for (a) **1c**, (b) **2c**, (c) **3c** and (d) **4c**.

Figure S11. Phosphorescence spectra in optically matched (λ_{ex} = 266 nm, $A^{266\ nm}$ = 0.4) **1c**, **2c**, and **3c** glassy ethanol matrix measured at 77 K. The spectrum of **2c** was 10 times multiplied.

Figure S12. Optimized structures at the ground state of **1a**, **2a**, and **3a**.

Figure S13. Optimized structures at the triplet state of **1a**, **2a**, and **3a**.

Figure S14. Molecular orbitals at the T_1 state of **1a**, **2a** and **3a**.

Table S1. Cartesian coordinates for optimized structure at the ground state of **1a**.

Table S2. Cartesian coordinates for optimized structure at the ground state of **2a**.

Table S3. Cartesian coordinates for optimized structure at the ground state of **3a**.

Table S4. Cartesian coordinates for optimized structure at the T_1 state of **1a**.

Table S5. Cartesian coordinates for optimized structure at the T_1 state of **2a**.

Table S6. Cartesian coordinates for optimized structure at the T_1 state of **3a**.

REFERENCES

1. Lepage, G. A. (1960) Incorporation of 6–thioguanine into nucleic acids. *Cancer Res.* **20**, 403–408.
2. Karran, P. and N. Attard (2008) Thiopurines in current medical practice: Molecular mechanisms and contributions to therapy–related cancer. *Nature* **8**, 24–36.
3. Rubin, Y. V., Y. P. Blagoi and V. A. Bokovoy (1995) 6–Thioguanine luminescence probe to study DNA and low–molecular–weight systems. *J. Fluoresc.* **5**, 263–272.
4. Qu, P., H. Lu, X. Ding, Y. Tao and Z. Lu (2009) Influences of urea and guanidine hydrochloride on the interaction of 6–thioguanine with bovine serum albumin. *Spectrochim. Acta. A Mol. Biomol. Spectrosc.* **74**, 1224–1228.
5. Massey, A., Y.-Z. Xu and P. Karran (2001) Photoactivation of DNA thiobases as a potential novel therapeutic option. *Curr. Biol.* **11**, 1142–1146.
6. Brem, R., F. Li and P. Karran (2009) Reactive oxygen species generated by thiopurine/UVA cause irreparable transcription–blocking DNA lesions. *Nucleic Acids Res.* **37**, 1951–1961.
7. Gay, L., M. R. Miller, P. B. Ventura, V. Devasthali, Z. Vue, H. L. Thompson, S. Temple, H. Zong, M. D. Cleary, K. Stankunas and C. Q. Doe (2013) Mouse TU tagging: A chemical/genetic intersectional method for purifying cell type–specific nascent RNA. *Genes Dev.* **27**, 98–115.
8. O'Donovan, P., C. M. Perrett, X. Zhang, B. Montaner, Y.-Z. Xu, C. A. Harwood, F. Hanaoka and P. Karran (2005) Azathioprine and UVA Light generate mutagenic oxidative DNA damage. *Science* **309**, 1871–1874.
9. Reelfs, O., Y.-Z. Xu, A. Massey, P. Karran and A. Storey (2007) Thiothymidine plus low–dose UVA kills hyperproliferative human skin cells independently of their human papilloma virus status. *Mol. Cancer Ther.* **6**, 2487–2495.
10. Lepage, G. A. and M. Jones (1961) Further studies on the mechanism of action of 6–thioguanine. *Cancer Res.* **21**, 1590–1594.
11. Ren, X., F. Li, G. Jeffs, X. Zhan, Y.-Z. Xu and P. Karran (2010) Guanine sulphinate is a major stable product of photochemical oxidation of DNA 6–thioguanine by UVA irradiation. *Nucleic Acids Res.* **38**, 1832–1840.
12. Pridgeon, S. W., R. Heer, G. A. Taylor, D. R. Newell, K. O'Toole, M. Robinson, Y.-Z. Xu, P. Karran and A. V. Boddy (2011) Thiothymidine combined with UVA as a potential novel therapy for bladder cancer. *Br. J. Cancer* **104**, 1869–1876.

13. Reelfs, O., P. Karran and A. R. Young (2012) 4–Thiothymidine sensitization of DNA to UVA offers potential for a novel photochemotherapy. *Photochem. Photobiol. Sci.* **11**, 148–154.
14. Boulnois, J. L. (1986) Photophysical processes in recent medical laser developments: A review. *Lasers Med. Sci.* **1**, 47–66.
15. Sanli, S., Y. Altun and G. Guven (2014) Solvent effects on pK_a values of some anticancer agents in acetonitrile−water binary mixtures. *J. Chem. Eng. Data* **59**, 4015–4020.
16. Eccleston, J. F. and P. M. Bayley (1980) Circular dichroic spectra of 6–thioguanosine nucleotides and their complexes with myosin subfragment. *Biochemisty* **19**, 5050–5056.
17. Reichardt, C., C. Guo and C. E. Crespo-Hernández (2011) Excited–state dynamics in 6–thioguanosine from the femtosecond to microsecond time scale. *J. Phys. Chem. B* **115**, 3263–3270.
18. Pollum, M., L. A. Ortiz-Rodríguez, S. Jockusch and C. E. Crespo-Hernández (2016) The triplet state of 6–thio–2′–deoxyguanosine: Intrinsic properties and reactivity toward molecular oxygen. *Photochem. Photobiol.* **92**, 286–292.
19. Zhang, Y., X. Zhu, J. Smith, M. T. Haygood and R. Gao (2011) Direct observation and quantitative characterization of singlet oxygen in aqueous solution upon UVA excitation of 6–thioguanines. *J. Phys. Chem. B* **115**, 1889–1894.
20. Holmes, R. E. and R. K. Robins (1964) Purine nucleosides. VII. Direct bromination of adenosine, deoxyadenosine, guanosine, and related purine nucleosides. *J. Am. Chem. Soc.* **86**, 1242–1245.
21. Michael, M. A., H. B. Cottam, D. F. Smee, R. K. Robins and G. D. Kini (1993) Alkylpurines as immunopotentiating agents. Synthesis and antiviral activity of certain alkylguanines. *J. Med. Chem.* **36**, 3431–3436.
22. Gerster, J. F., B. C. Hinshaw, R. K. Robins and L. B. Townsed (1968) Purine nucleosides. XIX. The synthesis of certain 8–chloropurine nucleosides and related derivatives. *J. Org. Chem.* **33**, 1070–1073.
23. Bookser, B. C. and N. B. Raffaele (2007) High–throughput five minute microwave accelerated glycosylation approach to the synthesis of nucleoside libraries. *J. Org. Chem.* **72**, 173–179.
24. Jayanth, N., S. Ramachandran and M. Puranik (2009) Solution structure of the DNA damage lesion 8–oxoguanosine from ultraviolet resonance Raman spectroscopy. *J. Phys. Chem. A* **113**, 1459–1471.
25. Zhang, Y., J. Dood, A. Beckstead, J. Chen, X. Li, C. J. Burrows, Z. Lu, S. Matsika and B. Kohler (2013) Ultrafast excited–state dynamics and vibrational cooling of 8–oxo–7, 8–dihydro–2′–deoxyguanosine in D_2O. *J. Phys. Chem. A* **117**, 12851–12857.
26. Lu, Z., A. A. Beckstead, B. Kohler and S. Matsika (2015) Excited state relaxation of neutral and basic 8–oxoguanine. *J. Phys. Chem. B* **119**, 8293–8301.
27. Harada, Y., T. Suzuki, T. Ichimura and Y.-Z. Xu (2007) Triplet formation of 4–thiothymidine and its photosensitization to oxygen studied by time–resolved thermal lensing technique. *J. Phys. Chem. B* **111**, 5518–5524.
28. Kuramochi, H., T. Kobayashi, T. Suzuki and T. Ichimura (2010) Excited–state dynamics of 6–aza–2–thiothymine and 2–thiothymine: Highly efficient intersystem crossing and singlet oxygen photosensitization. *J. Phys. Chem. B* **114**, 8782–8789.
29. Suzuki, T., S. Miyata and T. Isozaki (2015) Absorption spectra of 8–oxoguanosine and 8–thioguanosine. *Photomed. Photobiol.* **37**, 21–22.
30. Pollum, M., S. Jockusch and C. E. Crespo-Hernández (2014) 2,4–Dithiothymine as a potent UVA chemotherapeutic agent. *J. Am. Chem. Soc.* **136**, 17930–17933.
31. Pollum, M., S. Jockuschb and C. E. Crespo-Hernández (2015) Increase in the photoreactivity of uracil derivatives by doubling thionation. *Phys. Chem. Chem. Phys.* **17**, 27851–27861.
32. Haynes, W. M. (2011) *Handbook of Chemistry and Physics*, 92nd edn. CRC Press, Boca Raton, FL.
33. Frisch, M. J., G. W. Trucks, H. B. Schlegel, G. E. Scuseria, M. A. Robb, J. R. Cheeseman, G. Scalmani, V. Barone, B. Mennucci, G. A. Petersson, H. Nakatsuji, M. Caricato, X. Li, H. P. Hratchian, A. F. Izmaylov, J. Bloino, G. Zheng, J. L. Sonnenberg, M. Hada, M. Ehara, K. Toyota, R. Fukuda, J. Hasegawa, M. Ishida, T. Nakajima, Y. Honda, O. Kitao, H. Nakai, T. Vreven, J. A. Montgomery Jr, J. E. Peralta, F. Ogliaro, M. Bearpark, J. J. Heyd, E. Brothers, K. N. Kudin, V. N. Staroverov, T. Keith, R. Kobayashi, J. Normand, K. Raghavachari, A. Rendell, J. C. Burant, S. S. Iyengar, J. Tomasi, M. Cossi, N. Rega, J. M. Millam, M. Klene, J. E. Knox, J. B. Cross, V. Bakken, C. Adamo, J. Jaramillo, R. Gomperts, R. E. Stratmann, O. Yazyev, A. J. Austin, R. Cammi, C. Pomelli, J. W. Ochterski, R. L. Martin, K. Morokuma, V. G. Zakrzewski, G. A. Voth, P. Salvador, J. J. Dannenberg, S. Dapprich, A. D. Daniels, O. Farkas, J. B. Foresman, J. V. Ortiz, J. Cioslowski and D. J. Fox. (2013) *Gaussian 09, Revision D.01*. Gaussian, Inc., Wallingford, CT.
34. Gerster, J. F., J. W. Jones and R. K. Robins (1963) Purine nucleosides. IV. The synthesis of 6–halogenated 9–β–D–ribofuranosylpurines from inosine and guanosine. *J. Org. Chem.* **28**, 945–948.
35. Lewis, L. R., R. K. Robins and C. C. Cheng (1964) The preparation and antitumor properties of acylated derivatives of 6–thiopurine ribosides. *J. Med. Chem.* **7**, 200–204.
36. Rossi, R. R. and L. M. Lerner (1973) Specificity of inhibition of adenosine deaminase by trialcohols derived from nucleosides. *J. Med. Chem.* **16**, 457–460.
37. Naito, T., K. Ueno and F. Ishikawa (1964) Studies on nucleosides and nucleotides. VII. Synthesis of 2–amino–6–substituted–9–β–D–ribofuranosylpurines. *Chem. Pharm. Bull.* **12**, 951–954.
38. Ikaunieks, M. and M. Madre (2002) Reinvestigation of the reaction of 8–bromoguanine derivatives with sodium thiosulfate. *J. Chem. Res.* **8**, 226–227.
39. Golubeva, N. A. and A. V. Shipitsyn (2007) The synthesis of N^2, N^6–substituted diaminopurine ribosides. *Russ. J. Bioorg. Chem.* **33**, 562–568.
40. Torii, T., H. Shiragami, K. Yamashita, Y. Suzuki, T. Hijiya, T. Kashiwagi and K. Izawa (2006) Practical syntheses of penciclovir and famciclovir from N2–acetyl–7–benzylguanine. *Tetrahedron* **62**, 5709–5716.
41. Grünewald, C., T. Kwon, N. Piton, U. Főrster, J. Wachtveitl and J. W. Engels (2008) RNA as scaffold for pyrene excited complex. *Bioorg. Med. Chem.* **16**, 19–26.
42. Lin, T., J. Cheng, K. Ishiguro and A. C. Sartorelli (1985) 8–Substituted guanosine and 2′–deoxyguanosine derivatives as potential inducers of the differentiation of friend erythroleukemia cells. *J. Med. Chem.* **28**, 1194–1198.
43. Reitz, A. B., M. G. Goodman, B. L. Pope, D. C. Argentieri, S. C. Bell, L. E. Burr, E. Chourmouzis, J. Come, J. H. Goodman, D. H. Klaubert, B. E. Maryanoff, M. E. McDonnel, M. S. Rampulla, M. R. Schott and R. Chen (1994) Small–molecule immunostimulants. Synthesis and activity of 7,8–disubstituted guanosines and structurally related compounds. *J. Med. Chem.* **37**, 3561–3578.
44. Zhang, X., J. Wang and Y.-Z. Xu (2013) Systematic assignment of NMR spectra of 5–substituted–4–thiopyrimidine nucleosides. *Magn. Reson. Chem.* **51**, 523–529.
45. Zhang, X. and Y.-Z. Xu (2011) NMR and UV studies of 4–thio–2′–deoxyuridine and its derivatives. *Molecules* **16**, 5655–5664.
46. Isozaki, T., J. Ikemi and T. Suzuki (2012) Multi–photon excitation studies of 6–thioguanosine as a potential agent for photodynamic therapy. *Photomed. Photobiol.* **34**, 67–68.
47. Isozaki, T., S. Ando and T. Suzuki. Simultaneous two–photon absorption of thioguanosine analogue 2′,3′,5′–tri–*O*–acetyl–6,8–dithioguanosine with its potential application to photodynamic therapy. In preparation.
48. Stewart, M. J., J. Leszczynski, Y. V. Rubin and Y. P. Blagoi (1997) Tautomerism of thioguanine: From gas phase to DNA. *J. Phys. Chem. A* **101**, 4753–4760.
49. Rodgers, M. A. J. (1983) Solvent–induced deactivation of singlet oxygen: Additivity relationships in nonaromatic solvents. *J. Am. Chem. Soc.* **105**, 6201–6205.
50. Clennan, E. L., L. J. Noe, T. Wen and E. Szneler (1989) Solvent effects on the ability of amines to physically quench singlet oxygen as determined by time–resolved infrared emission studies. *J. Org. Chem.* **54**, 3584–3587.
51. Martí, C., O. Jürgens, O. Cuenca, M. Casals and S. Nonell (1996) Aromatic ketones as standards for singlet molecular oxygen O_2 ($^1\Delta_g$) photosensitization. Time–resolved photoacoustic and near–IR emission studies. *J. Photochem. Photobiol., A* **97**, 11–18.
52. Schweitzer, C. and R. Schmidt (2003) Physical mechanisms of generation and deactivation of singlet oxygen. *Chem. Rev.* **103**, 1685–1758.